

# Reassessing spin-coupled (full generalized valence bond) descriptions of ozone using three-center bond indices

David L. Cooper<sup>a,\*</sup>, Fabio E. Penotti<sup>b</sup>, Robert Ponec<sup>c</sup>

<sup>a</sup> *Department of Chemistry, University of Liverpool, Liverpool L69 7ZD, United Kingdom*

<sup>b</sup> *Consiglio Nazionale delle Ricerche, Istituto di Scienze e Tecnologie Molecolari, Via Golgi 19, I-20133 Milano MI, Italy*

<sup>c</sup> *Institute of Chemical Process Fundamentals, Academy of Sciences of the Czech Republic v.v.i., Rozvojová 135, 165 02 Prague 6, Czech Republic*

\* **Corresponding Author.** E-mail: dlc@liverpool.ac.uk

## ABSTRACT

Domain-averaged Fermi hole analysis is carried out for the ground state of O<sub>3</sub> at its equilibrium geometry using a complete-active-space self-consistent field CASSCF(18,14) wavefunction, based on a slightly expanded full-valence active space. This initial analysis is augmented with an examination of the corresponding localized natural orbitals (LNOs) and of the numerical values obtained with a new improved definition of three-center bond indices for correlated singlet systems. Much the same pattern of LNOs is observed when using instead a subsequent internally-contracted multiconfiguration-reference configuration interaction construction, which also provides very similar values for the three-center bond indices. This gives us confidence to use such bond indices, alongside relative energies and the electric dipole moment, to assess the relative merits of various combinations of spin-coupled (full generalized valence bond) components with ten active electrons: four  $\pi$ , four  $\sigma$  bonding and the two nonbonding  $\sigma$  electrons associated with the central O atom. These multi-component valence bond descriptions were generated either with or without subsequent orbital reoptimization. The description of the  $\pi$  system which emerges from all of our analysis conforms to a standard model of three-center four-electron  $\pi$  bonding that incorporates a nontrivial degree of (partial) diradical character. Whereas certain combinations of ten-electron spin-coupled components can faithfully reproduce such a picture, none of the individual rival components appears to have sufficient flexibility on its own.

Keywords:  $\pi$  system in O<sub>3</sub>; Full-GVB and spin-coupled; QTAIM-generalized three-center bond index; Domain-averaged Fermi holes; Localized natural orbitals.

## 1. Introduction

Whereas introductory texts typically describe the ozone three-center four-electron  $\pi$  system in terms of resonance between the zwitterionic Lewis structures **1a** and **1b** (see Fig. 1), there is a fair amount of evidence in favor of partial diradical character, as might be represented by structure **1d**. Additionally, by analogy to  $\text{SO}_2$ , we may also envisage the possible participation of the Lewis-like structure **1c**. In keeping with the existence of these different representations, it is well-established that *ab initio* electronic structure calculations based on spin-coupled (SC) theory, also known as the full-generalized valence bond (full-GVB) approach, yield rival solutions for the electronic ground state of  $\text{O}_3$  at its equilibrium geometry that appear to be qualitatively somewhat different from one another, even though they are energetically rather close. One such solution,  $\text{SC}_d$ , features a diradical-like  $\pi$  system (cf. structure **1d**) whereas in the other case,  $\text{SC}_c$ , the  $\pi$  system appears at first sight to be more reminiscent of the ‘closed-shell’ description of  $\text{SO}_2$  (cf. structure **1c** although, as will be shown later, there are significant deviations from two fully-formed  $\pi$  bonds). The existence of these two closely-competing descriptions first emerged in  $\text{SC}(4)$  calculations [1], in which only the four electrons of the  $\pi$  system were treated as active, but Takeshita et al. [2] showed subsequently that much the same situation occurs when using  $\text{SC}(8)$  solutions, in which the four electrons that describe the  $\sigma$  bonding were also included in the active space.

«Fig. 1 near here»

In previous work, in which Penotti and Cooper [3] constructed also a two-configuration pseudo-ionic description  $\text{SC}_I(4)$  (cf. the resonance between structures **1a** and **1b** in Fig. 1) and then examined various combinations of  $\text{SC}_c(4)$ ,  $\text{SC}_d(4)$  and  $\text{SC}_I(4)$  components (with or without further orbital reoptimization), it was shown that neither of the  $\text{SC}_c(4)$  nor  $\text{SC}_d(4)$  solutions provides a satisfactory description on its own. Such an outcome, in which no particular SC (or full-GVB) description emerges as being the preferred one for ozone, is of course somewhat disappointing. Additionally, it was shown that although the  $\text{SC}_I(4)$  wavefunction was entirely inadequate on its own, it could be of some value when combined with other solutions [3].

We reopen the problem of ozone in the present work, first extracting descriptions of its electronic structure from appropriate complete-active-space self-consistent field (CASSCF) calculations by means of the analysis of domain-averaged Fermi holes (DAFHs) [4-13] and of localized natural orbitals (LNOs), as well as the computation of certain two- and three-center bonding indices. Direct comparison is made with the analysis of an

analogous internally-contracted multiconfiguration-reference configuration interaction (icMRCI) construction, thereby demonstrating that the CASSCF wavefunction already captures the key qualitative features of the  $\sigma$  and  $\pi$  systems. The various numerical results can then be used with confidence to assess the relative quality of (combinations of)  $SC_x(10)$  components ( $x=c, d, I$ ) in which the active space used by Takeshita et al. [2] is expanded so as to include also the two nonbonding  $\sigma$  valence electrons associated with the central O atom.

Our various calculations also enable a reassessment of the (disputed) assertions of Kalemos and Mavridis [14-16] that  $O_3$  is a genuine closed-shell system that lacks significant diradical character. Of course, most previous studies, including an examination of oriented quasi-atomic molecular orbitals [17], analyses of CASSCF and icMRCI wavefunctions [18, 19], VB calculations based on so-called strictly localized orbitals [20, 21], considerations of increased-valence structures [22, 23], and various full-GVB or SC studies [1-3, 24], have tended to support the more conventional ‘partial diradical’ interpretation of the bonding in this molecule.

## 2. Computational framework

The orbitals of the  $\sigma$  system of ozone do of course transform as  $A_1$  and  $B_2$  in  $C_{2v}$  symmetry, whereas the  $\pi$  system corresponds to  $B_1$  and  $A_2$ . A key difference between the  $SC_c$  and  $SC_d$  solutions is that the two sets of  $\pi$  orbitals span  $2 \times B_1 + 2 \times A_2$  and  $3 \times B_1 + 1 \times A_2$ , respectively. A full-valence CASSCF(18,12) expansion for ozone involves all symmetry-allowed distributions of the 18 valence electrons in a total of 12 orbitals, even though the  $\pi$  space corresponds only to  $2 \times B_1 + 1 \times A_2$ . With this limitation in mind, we chose to generate CASSCF(18,14) wavefunctions, in which the full-valence active space is expanded by  $B_1 + A_2$ , so as to encompass the flexibility that is inherent in the  $\pi$  spaces of the  $SC_c$  and  $SC_d$  solutions. We also subsequently calculated an icMRCI wavefunction based on CASSCF(18,14) as its reference. (For the purposes of comparison, we also carried out full-valence CASSCF(18,12) and subsequent icMRCI calculations.)

As has been described many times before, domain-averaged Fermi hole (DAFH) analysis [4-13] for a chosen domain  $\Omega$  involves the construction of a matrix representation  $G_\Omega$  of the so-called domain-averaged ‘hole’,  $g_\Omega(\mathbf{r})$ , which can be defined according to

$$g_\Omega(\mathbf{r}_1) = \rho(\mathbf{r}_1) \int_\Omega \rho(\mathbf{r}_2) d\mathbf{r}_2 - 2 \int_\Omega \rho(\mathbf{r}_1, \mathbf{r}_2) d\mathbf{r}_2 \quad (1)$$

The quantities  $\rho(\mathbf{r}_1)$  and  $\rho(\mathbf{r}_1, \mathbf{r}_2)$  which appear in this expression are the ordinary spinless first-order electron density and the pair density, respectively, but the majority of applications to date have used wavefunctions that are based exclusively on doubly-occupied orbitals (whether SCF or Kohn-Sham), thereby avoiding the requirement for  $\rho(\mathbf{r}_1, \mathbf{r}_2)$  to be available. Nevertheless, an increasing number of studies (including this one) have used Eq. (1) directly for more general correlated descriptions, such as those from CASSCF and SC calculations, expressing the wavefunctions as natural orbital expansions with non-integer occupation numbers ( $\omega_i$ ), and making explicit use of the correlated pair density matrix. Each  $\mathbf{G}_\Omega$  matrix, conveniently expressed in the basis of the canonical natural orbitals ( $\phi_i$ ), is typically constructed for the active space of the relevant calculation. In the next step of the analysis, the eigenvalues and eigenvectors of the  $\mathbf{G}_\Omega$  matrix for a given domain  $\Omega$  are subjected to an implementation of the isopycnic localization procedure of Cioslowski [25], so as to re-express  $g_\Omega(\mathbf{r})$  in terms of so-called DAFH functions  $\varphi_i^\Omega$  with corresponding occupation numbers  $n_i^\Omega$ :

$$g_\Omega(\mathbf{r}) = \sum_i n_i^\Omega |\varphi_i^\Omega|^2 \quad (2)$$

The insights into correlated electronic structure that are provided by DAFH analysis are mostly extracted by examining pictorial depictions of the  $\varphi_i^\Omega$  functions, alongside their occupation numbers. A large body of evidence has shown that it can be particularly useful to identify each  $\Omega$  with an atomic domain that is generated by means of Bader's virial partitioning of the total electron density, *i.e.* to use the quantum theory of atoms in molecules (QTAIM) [26]. This is the approach that we follow here and so the DAFH analysis can be expected to give a clear indication of the broken or dangling valences that are created by notionally splitting bonds, so as to formally isolate the given 'atom' from the rest of the molecule, as well as to provide information about the electron pairs that remain intact within a given QTAIM domain.

Alongside the natural orbital representation ( $\phi_i, \omega_i$ ) of a given wavefunction and the availability of its pair density matrix expressed in this basis, QTAIM-based DAFH analysis also requires the full set of domain-condensed overlaps:

$$\langle \phi_I | \phi_J \rangle_\Omega = \int_\Omega \phi_I(\mathbf{r}) \phi_J(\mathbf{r}) d\mathbf{r} \quad (3)$$

Such quantities are readily available when performing QTAIM analysis. Of course, instead of identifying  $\Omega$  with a single QTAIM domain, we could choose to use instead the union of multiple QTAIM domains. In the special case that  $\Omega$  is taken to be the union of all such domains, so that it corresponds to the whole molecule, then  $\mathbf{G}_\Omega$  becomes the diagonal matrix with elements  $\omega_I$ . As a consequence, DAFH analysis for an entire molecule is formally equivalent to subjecting the canonical natural orbitals  $\phi_I$  to Cioslowski's isopycnic transformation procedure [25], so as to generate a set of localized natural orbitals (LNOs).

The  $\text{SC}_c(10)$  and  $\text{SC}_d(10)$  valence bond (VB) wavefunctions considered in the present work take the following general form:

$$\Psi_{\text{SC}_c(10)} = \hat{\mathcal{A}} \left[ \left( \prod_{i=1}^7 \kappa_i \alpha \kappa_i \beta \right) \left( \prod_{\mu=1}^6 \sigma_\mu \right) \left( \prod_{\nu=1}^4 \pi_\nu \right) \left( \sum_{k=1}^{42} c_k \Theta_k^{10} \right) \right] \quad (4)$$

in which the singly-occupied nonorthogonal active orbitals  $\sigma_\mu$  and  $\pi_\nu$  have been denoted according to their symmetries and the  $\Theta_k^{10}$  are the full set of Kotani spin functions for a ten-electron singlet system [27] (vide infra). The doubly-occupied inactive orbitals  $\kappa_i$ , which accommodate the essentially  $\text{O}(1s^2)$  cores and the nonbonding  $\sigma$  electrons on the two terminal atoms, were obtained by means of a Boys localization of a CASSCF(4,3) wavefunction. The inactive orbitals  $\kappa_i$  were then kept fixed in the  $\text{SC}(10)$  calculations, whereas the various  $\sigma_\mu$  and  $\pi_\nu$  active orbitals and the spin-coupling coefficients,  $c_k$ , were simultaneously freely optimized, being subject only to any symmetry requirements.

Kotani spin functions are in principle constructed sequentially by coupling each time the spin of a single electron to the total spin of a group of  $n < N$  electrons according to the usual rules for combining angular momenta. A branching diagram, as shown in Fig. 2, provides a straightforward means of visualizing such spin functions as rightwards paths from the origin to the required combination of  $N$  and  $S$ . The values in the circles are the total numbers of such paths and thus the dimensions of the full spin spaces for a given  $N$  and  $S$ . As a shorthand for a given path, we may use the symbols  $\alpha$  for a rightwards step up and  $\beta$  for a corresponding single-electron step down. The lowest path for a ten-electron singlet system, denoted  $\alpha\beta\alpha\beta\alpha\beta\alpha\beta$ , represents the perfect-pairing mode of spin coupling and it coincides with the corresponding function in the Rumer basis; it is the last function ( $k=42$ ) in the standard ordering of Kotani spin functions [27].

«Fig. 2 near here»

For the corresponding pseudo-ionic  $SC_I(10)$  construction (cf. the resonance between structures **1a** and **1b** in Fig. 1), we optimized instead a wavefunction consisting of two configurations which transform into one another under reflection in the  $\sigma_v(xz)$  mirror plane. In either of these configurations, two of the  $\pi$  orbitals were expanded only in terms of basis functions on one of the terminal atoms and the other two  $\pi$  orbitals were restricted only to use basis functions associated with the other two atoms. There were no such restrictions on the active  $\sigma$  orbitals in a given configuration. The resulting two-configuration  $SC_I(10)$  wavefunction, featuring different but symmetry-related sets of  $\sigma$  orbitals, should in principle have sufficient flexibility so as to be able to provide a representation of the model suggested by Kalemios and Mavridis [14], were it to be energetically favored. Those authors described  $O_3$  as a genuine closed-shell singlet species that is notionally formed from a combination of  $O_2(a^1\Delta_g)$  and  $O(^1D)$  excited states (using dative bonding).

In order to quantify certain aspects of the bonding in the  $\sigma$  and  $\pi$  systems of ozone, whether using CASSCF, icMRCI or VB wavefunctions, it proves useful in the present work to use particular definitions of two- and three-center indices that are closely related to one another. A useful starting point is the following definition of a basic two-center Wiberg-Mayer bond index,  $W_{AB}$  [28]:

$$W_{AB} = \sum_{\mu \in A} \sum_{\nu \in B} [(\mathbf{PS})_{\mu\nu}(\mathbf{PS})_{\nu\mu} + (\mathbf{P}^s\mathbf{S})_{\mu\nu}(\mathbf{P}^s\mathbf{S})_{\nu\mu}] \quad (5)$$

in which  $\mathbf{P}$ ,  $\mathbf{P}^s$  and  $\mathbf{S}$  are the spinless one-electron density matrix, spin-density matrix and overlap matrix, respectively, and the notation  $\mu \in A$  signifies that the relevant summation is restricted to the basis functions associated with atomic center  $A$ . Mayer has suggested for singlet correlated systems that the spin-density matrix  $\mathbf{P}^s$  should be substituted by a matrix  $\mathbf{R}$ , so that Eq. (5) becomes [29]:

$$W_{AB} = \sum_{\mu \in A} \sum_{\nu \in B} [(\mathbf{PS})_{\mu\nu}(\mathbf{PS})_{\nu\mu} + (\mathbf{RS})_{\mu\nu}(\mathbf{RS})_{\nu\mu}] \quad (6)$$

in which the matrix  $\mathbf{R}$  is defined by the following sequence [29]:

$$\begin{aligned}
\mathbf{uS} &= 2\mathbf{PS} - (\mathbf{PS})^2 \\
\mathbf{u}^\lambda &= \mathbf{S}^{1/2}(\mathbf{uS})\mathbf{S}^{-1/2} \\
\mathbf{R} &= \mathbf{S}^{-1/2}(\mathbf{u}^\lambda)^{1/2}\mathbf{S}^{-1/2}
\end{aligned}
\tag{7}$$

When they are expressed in the basis of (real) orthonormal natural orbitals  $\phi_I$  with corresponding occupation numbers  $\omega_I$ , the matrices  $\mathbf{P}$  and  $\mathbf{R}$  are diagonal, with elements  $\omega_I$  and  $R_{II} = [\omega_I(2 - \omega_I)]^{1/2}$ , respectively, and  $\mathbf{S}$  is of course a unit matrix. As a consequence, the corresponding QTAIM-generalized [30] Wiberg-Mayer index for a correlated singlet system [29] takes the following simple form [13]:

$$W_{AB} = \sum_I \sum_J (\omega_I \omega_J + R_{II} R_{JJ}) \langle \phi_I | \phi_J \rangle_{\Omega_A} \langle \phi_I | \phi_J \rangle_{\Omega_B}
\tag{8}$$

This is the specific definition of  $W_{AB}$  that was used in the present work. Note that the sum of all possible  $W_{AB}$  values is necessarily equal to the total number of electrons. Furthermore, in the special case of a planar molecule such as ozone, we may identify the separate contributions from the  $\sigma$  and  $\pi$  systems to the total value of  $W_{AB}$ .

It is straightforward to write down the three-center analogue of Eq. (5) [28], to replace  $\mathbf{P}^s$  by  $\mathbf{R}$  [29] in the case of a correlated singlet system, to switch to the basis of natural orbitals and then to construct the QTAIM generalization of this index [31, 32]. This leads to the following definition:

$$X_{ABC} = \frac{1}{4} \sum_I \sum_J \sum_K \left( \begin{aligned} &\omega_I \omega_J \omega_K + \omega_I R_{JJ} R_{KK} \\ &+ R_{II} \omega_J R_{KK} + R_{II} R_{JJ} \omega_K \end{aligned} \right) \langle \phi_I | \phi_K \rangle_{\Omega_A} \langle \phi_I | \phi_J \rangle_{\Omega_B} \langle \phi_J | \phi_K \rangle_{\Omega_C}
\tag{9}$$

However, in the present work, we have chosen to use instead a new, alternative approach that takes its inspiration from the specific forms of Eqs. (5)–(8). In particular, we consider an index  $Y_{ABC}$  that takes the following form:

$$\begin{aligned}
Y_{ABC} &= \frac{1}{8} \sum_{\mu \in A} \sum_{\nu \in B} \sum_{\lambda \in C} [(\mathbf{PS})_{\mu\nu} (\mathbf{PS})_{\nu\lambda} (\mathbf{PS})_{\lambda\mu} + (\mathbf{QS})_{\mu\nu} (\mathbf{QS})_{\nu\lambda} (\mathbf{QS})_{\lambda\mu}] \\
&+ \frac{1}{8} \sum_{\mu \in A} \sum_{\nu \in C} \sum_{\lambda \in B} [(\mathbf{PS})_{\mu\nu} (\mathbf{PS})_{\nu\lambda} (\mathbf{PS})_{\lambda\mu} + (\mathbf{QS})_{\mu\nu} (\mathbf{QS})_{\nu\lambda} (\mathbf{QS})_{\lambda\mu}]
\end{aligned}
\tag{10}$$

in which the matrix  $\mathbf{Q}$  is defined by the following sequence:

$$\begin{aligned}
 \mathbf{tS} &= 4\mathbf{PS} - (\mathbf{PS})^3 \\
 \mathbf{t}^\lambda &= \mathbf{S}^{3/2}(\mathbf{tS})\mathbf{S}^{-1/2} \\
 \mathbf{Q} &= \mathbf{S}^{-1/2}(\mathbf{t}^\lambda)^{1/3}\mathbf{S}^{-1/2}
 \end{aligned}
 \tag{11}$$

Working in the basis of (real) orthonormal natural orbitals  $\phi_I$  with occupation numbers  $\omega_I$ , the matrix  $\mathbf{Q}$  turns out to be diagonal, with elements  $Q_{II} = [\omega_I(2 + \omega_I)(2 - \omega_I)]^{1/3}$ , so that the QTAIM generalization of Eq. (10) takes the following simple form:

$$Y_{ABC} = \frac{1}{4} \sum_I \sum_J \sum_K (\omega_I \omega_J \omega_K + Q_{II} Q_{JJ} Q_{KK}) \langle \phi_I | \phi_K \rangle_{\Omega_A} \langle \phi_I | \phi_J \rangle_{\Omega_B} \langle \phi_J | \phi_K \rangle_{\Omega_C}
 \tag{12}$$

Note that the various permutations of the three indices necessarily yield identical values of  $Y_{ABC}$ , and so it is more convenient when all three indices are different to quote instead a single value of  $Y(A,B,C) = 3! Y_{ABC}$ . Comparing Eqs. (8) and (12), and similarly Eqs. (7) and (11), it is clear that our chosen two- and three-center bond index definitions are closely related to one another, as desired. Another distinct advantage of this particular formulation is that the sum of all possible  $Y_{ABC}$  values is equal to the total number of electrons, essentially by construction. The same is not true of the sum of all possible  $X_{ABC}$  values, although we do find for a number of correlated singlet systems, including ozone, that the value of  $Y(A,B,C)$  for a given triad usually only differs from  $X(A,B,C) = 3! X_{ABC}$  in the third decimal place. As was the case for  $W_{AB}$ , defined by Eq. (8), the form of Eq. (12) allows us to identify for a planar molecule such as ozone the separate contributions to the total value of  $Y_{ABC}$  from the  $\sigma$  and  $\pi$  systems. (For all cases that we quote values of  $Y(\text{O1},\text{O2},\text{O3})$  in this paper, the corresponding values of  $X(\text{O1},\text{O2},\text{O3})$  are shown in Table S2 in the Supplementary Material.)

The majority of the CASSCF calculations [33, 34] and all of the icMRCI calculations [35, 36] were carried out using the MOLPRO package [37, 38]. QTAIM analysis [26] of total electron densities was performed using AIMAll [39], with the DAFH analysis, generation of LNOs and calculation of bond indices carried out for the active spaces of the various wavefunctions using our own codes. All of the  $\text{SC}_x(10)$  wavefunctions, as well as various combinations of them, were calculated using the generalized multiconfiguration spin-coupled (GMCS) program developed by Penotti [40-43]. Integrals over basis functions and the Boys-localized CASSCF(4,3) inactive orbitals that were required for these GMCS



calculations were generated using the GAMESS-US package [44, 45]. All of the wavefunction calculations were carried out at an experimentally-derived geometry [46] ( $r_{\text{OO}} = 1.2716 \text{ \AA}$  and  $\theta = 117.47^\circ$ ) using standard cc-pVQZ Gaussian basis sets in spherical form. When assessing the relative weights of different components in our various VB wavefunctions, we employed both the Chirgwin-Coulson [47] and Gallup-Norbeck [48] definitions. Pictorial depictions of DAFH functions, LNOs and SC active orbitals were produced from Virtual Reality Markup Language (VRML) files that were generated using MOLDEN [49].

### 3. Results and discussion

#### 3.1. CASSCF(18,14) description

It is useful to start with an examination of the localized natural orbitals (LNOs) that are generated by applying the isopycnic localization procedure to the canonical natural orbitals of the CASSCF(18,14) wavefunction. As can be seen from Fig. 3, there are four almost doubly-occupied nonbonding  $\sigma$  LNOs ( $\psi_1$ ,  $\psi_2$ ,  $\psi_4$  and  $\psi_5$ ) on the terminal O atoms, one almost doubly-occupied nonbonding  $\sigma$  function ( $\psi_3$ ) on the central atom and two symmetry-equivalent almost doubly-occupied two-center  $\sigma$  bonding orbitals ( $\psi_6$  and  $\psi_7$ ). As such, this description of the  $\sigma$  system corresponds rather well to two rather ordinary two-center two-electron O–O  $\sigma$  bonds plus the anticipated pattern of nonbonding  $\sigma$  orbitals. Two further symmetry-related  $\sigma$  LNOs ( $\psi_{11}$  and  $\psi_{12}$ ), not shown in Fig. 3, have occupations of just 0.06 each.

«Fig. 3 near here»

The corresponding description of the  $\pi$  system is, however, not so immediately straightforward. As can be seen from Fig. 3, LNO  $\psi_8$  (occupancy 1.52) is clearly a three-center  $\pi$  function, but with its strongest allegiance to the central O atom, whereas  $\psi_9$  and  $\psi_{10}$  (occupancy 1.23 each) are two symmetry-equivalent mostly two-center  $\pi$  functions, but with a small out-of-phase component on the opposing terminal atom. Such a pattern of  $\pi$  LNOs is suggestive of three-center four-electron  $\pi$  bonding and so, in order to gain further insight, we turn now to the DAFH analysis of this CASSCF(18,14) wavefunction before examining the corresponding values of the three-center index  $Y$  for the  $\sigma$  and  $\pi$  systems. (As was mentioned earlier, we also analyzed an icMRCI construction based on CASSCF(18,14) as its reference. The LNOs for this icMRCI wavefunction, which are shown in Fig. S1 in the

Supplementary Material, are very difficult to distinguish by eye from those for the CASSCF(18,14) wavefunction, but there are small changes to the occupation numbers.)

DAFH functions for the domain of the central atom (O1) are depicted in the first column of Fig. 4, together with their occupation numbers, and the corresponding functions and occupation numbers for the domain of one of the terminal atoms (O2) are shown in the second column. We observe for the O1 domain a pair of symmetry-equivalent two-center  $\sigma$  functions ( $\varphi_3^{01}$  and  $\varphi_4^{01}$ ) with occupancy 1.13 which can be considered as the broken or dangling valences of the two formally split O–O  $\sigma$  bonds. Clearly associated with these two functions are the symmetry-equivalent functions  $\varphi_4^{02}$  and  $\varphi_4^{03}$  (occupation 0.91 each) which emerge from the DAFH analysis for the domain of the respective terminal atom. Taken together, the forms and complementary occupation numbers of  $\varphi_3^{01}$ ,  $\varphi_4^{01}$ ,  $\varphi_4^{02}$  and  $\varphi_4^{03}$  are strongly suggestive of two approximately doubly-occupied two-center O–O  $\sigma$  bonds.

«Fig. 4 near here»

For each of the three QTAIM domains, the DAFH function with the highest occupation takes the form of an almost doubly-occupied nonbonding  $\sigma$  function that is localized in the respective domain. These  $\sigma$  functions resemble very closely the corresponding  $\sigma$  LNOs shown in Fig. 3. Indeed, the overlaps  $\langle \varphi_1^{01} | \psi_3 \rangle$  and  $\langle \varphi_1^{02} | \psi_1 \rangle = \langle \varphi_1^{03} | \psi_2 \rangle$  exceed 0.999. DAFH analysis for the O2 domain also produces a nonbonding  $2p_\sigma$ -like function ( $\varphi_2^{02}$ , occupation 1.89) that has an overlap with LNO  $\psi_4$  that exceeds 0.999. All in all, the DAFH analysis of the CASSCF(18,14) wavefunction corresponds fairly closely to our usual notions of two rather ordinary two-center two-electron  $\sigma$  bonds, alongside the anticipated pattern of nonbonding  $\sigma$  electrons. On the other hand, just as was the case for the LNOs, the corresponding DAFH-based description of the  $\pi$  system is, again, less straightforward.

We observe from Fig. 4 a DAFH  $\pi$  function ( $\varphi_2^{01}$ ) for the O1 domain (occupation 1.35) that closely resembles LNO  $\psi_8$  and a  $\pi$  function ( $\varphi_3^{02}$ ) for the O2 domain (occupation 1.21) that closely resembles LNO  $\psi_9$ . The overlaps  $\langle \varphi_2^{01} | \psi_8 \rangle$  and  $\langle \varphi_3^{02} | \psi_9 \rangle = \langle \varphi_3^{03} | \psi_{10} \rangle$  are 0.999. The only other  $\sigma$  or  $\pi$  DAFH function with an occupation greater than 0.09 is for the domain of O1; it takes the form of the out-of-phase (antibonding) combination of  $2p_\pi$  functions on the terminal atoms, each deformed towards the central atom, but the occupation of  $\varphi_5^{01}$  is just 0.14. Taken together, the forms and occupation numbers of DAFH functions  $\varphi_2^{01}$ ,  $\varphi_3^{02}$ ,  $\varphi_3^{03}$  and  $\varphi_5^{01}$  (as well as those of LNOs  $\psi_8$ ,  $\psi_9$  and  $\psi_{10}$ ) are strongly suggestive of

three-center four-electron  $\pi$  bonding in this molecule. As such, we should expect the value of  $Y(\text{O1},\text{O2},\text{O3})$  for the  $\pi$  system to be negative [50, 51].

Values of the two-center QTAIM-generalized Wiberg-Mayer index  $W_{AB}$  (Eq. (8)) and of the three-center index  $Y(\text{O1},\text{O2},\text{O3})$  are reported in Table 1, together with the total energies and the computed electric dipole moments. In addition to the CASSCF(18,14) wavefunction itself, we also analyzed an icMRCI wavefunction based on CASSCF(18,14) as its reference. Results are also reported in Table 1 for the corresponding CASSCF(4,5) wavefunction in which all of the  $\sigma$  orbitals are inactive and the  $\pi$  active space spans  $3 \times B_1 + 2 \times A_2$  (*i.e.* the full-valence  $\pi$  space expanded by  $B_1 + A_2$ ). (The corresponding results for CASSCF(4,3) (full-valence  $\pi$ ) and for CASSCF(18,12) (full-valence) descriptions are available in Table S1 in the Supplementary Material, alongside the values obtained from an icMRCI expansion based on CASSCF(18,12) as its reference. Comparing Table 1 with Table S1, we notice that whereas the icMRCI wavefunction that is based on CASSCF(18,14) gives a dipole moment of 0.510 D, the corresponding construction based on CASSCF(18,12) gives 0.537 D, which is closer to the experimentally-derived value of 0.53373 D [46], but the total energy is poorer. Using the same geometry and basis set, CCSD(T) (using CFOUR [52]) gives a dipole moment of 0.524 D; our two icMRCI calculations bracket this value.)

«Table 1 near here»

Looking first at the CASSCF(18,14) bond index values in Table 1, we observe a  $\sigma$ -only bond order between adjacent atoms ( $W_{12}$ ) of close to unity, with a much smaller value ( $W_{23}$ ) between the two terminal atoms. The  $\sigma$ -only value of  $Y(\text{O1},\text{O2},\text{O3})$  is fairly small, but negative, suggesting a small degree of three-center four-electron  $\sigma$  character that is consistent with the small  $\sigma$ -only value of  $W_{23}$ . The  $\pi$  system is clearly rather different, being characterized by  $\pi$ -only values of  $W_{12}$  and  $W_{23}$  that are somewhat closer to one another (*ca.* 0.43 and 0.24) and, correspondingly, a somewhat larger magnitude for the  $\pi$ -only value of  $Y(\text{O1},\text{O2},\text{O3})$  (*ca.* -0.14). Such a value of  $Y(\text{O1},\text{O2},\text{O3})$  is consistent with the significant degree of three-center four-electron  $\pi$  character that was suggested by the forms of the LNOs and by the results of the DAFH analysis.

Comparing the two final columns of Table 1, it is clear that the subsequent icMRCI calculations leads only to relatively small changes in any of the bond index values that we have considered. On the other hand, the CASSCF(4,5) construction, in which only the  $\pi$  system was included in the active space, gives smaller magnitudes for the corresponding  $\pi$ -only  $W$  and  $Y$  values, and the estimate of the dipole moment is particularly poor. The

occurrence of such large differences suggests that the dipole moment could be a useful quantity to monitor when comparing the various modern VB descriptions with one another. Given the apparently relatively ordinary nature of the  $\sigma$  system in ozone, it makes most sense when comparing the bond index values for these VB constructions to focus our attention on the variations in the  $\pi$ -only  $W$  and  $Y$  values.

### 3.2. Combining $SC_c(10)$ , $SC_d(10)$ and $SC_I(10)$ descriptions

Various numerical results for the  $SC_c(10)$ ,  $SC_d(10)$  and  $SC_I(10)$  wavefunctions are reported in Table 2. The total energies of the  $SC_c(10)$  and  $SC_d(10)$  descriptions turn out to be fairly similar to one another, with  $SC_c$  being slightly preferred, whereas it is clear that the  $SC_I(10)$  wavefunction is entirely inadequate on its own. This last observation is not consistent with the model suggested by Kalemos and Mavridis [14, 15] (*vide supra*).

Comparing Tables 1 and 2, we observe that the  $SC_c(10)$  and  $SC_d(10)$   $\pi$ -only values of  $W_{AB}$  and  $Y(O1,O2,O3)$  are fairly similar to the CASSCF(4,5) results while the corresponding values for  $SC_I(10)$  are somewhat more consistent with those from the CASSCF(18,14) and subsequent icMRCI wavefunctions. Whereas the  $SC_c(10)$  and  $SC_d(10)$  dipole moments are still too small, the  $SC_I(10)$  value is clearly far too large. All in all, none of the  $SC_c(10)$ ,  $SC_d(10)$  and  $SC_I(10)$  wavefunctions seems to be satisfactory on its own when they are all assessed from the joint perspectives of the  $\pi$ -only bond index values, the computed dipole moments and the relative energies. As a consequence, it seems worthwhile to consider also the relative merits of various combinations of these three wavefunctions.

For the most part, we consider here the variationally-determined combinations of the  $SC_c(10)$ ,  $SC_d(10)$  and  $SC_I(10)$  configurations in which all of the various spin-coupling coefficients are treated as free parameters, being subject only to any symmetry-induced constraints, but none of the orbitals are reoptimized. As such, it is important to start by examining the forms of the active spin-coupled orbitals in each of the separate SC configurations, so as to understand how they differ from one another. Comparing the orbitals shown in Fig. 5 for  $SC_c(10)$  (top two rows) with those for  $SC_d(10)$  (middle two rows), it is clear that the two sets of  $\sigma$  orbitals are fairly similar to one another and that the same is true, to a large extent, for the  $\pi$  orbitals localized on the terminal atoms. The main qualitative difference between these two sets of orbitals is thus for the two  $\pi$  orbitals that are formally associated with the central oxygen atom. For  $SC_c(10)$ , there are two symmetry-related predominantly  $p_\pi$  functions, with one deformed towards one terminal atom and one towards the other. For  $SC_d(10)$ , on the other hand, one of the  $\pi$  orbitals remains fairly localized on the

central atom whereas the other is clearly delocalized over all three centers. For the most part, the  $SC_c(10)$  and  $SC_d(10)$   $\pi$  orbitals are very reminiscent of those from earlier  $\pi$ -only  $SC_c(4)$  and  $SC_d(4)$  calculations [1-3]. Much the same is true of the  $SC_I(10)$   $\pi$  orbitals [3], but the symmetry-unique  $SC_I(10)$   $\sigma$  orbitals (see the final two rows of Fig. 5) do of course no longer transform into one another under the symmetry operations of the molecular point group, because of the (enforced) asymmetry in the  $\pi$  space. So, whereas the relative performance of the fixed-orbital combination of  $SC_c(10)$  with  $SC_d(10)$ , which we denote  $SC_c\oplus SC_d$ , will primarily be due to differences in the two sets of  $\pi$  orbitals, the corresponding combinations of  $SC_c(10)$  and/or  $SC_d(10)$  with  $SC_I(10)$  could also be sensitive to the differences in the descriptions of the  $\sigma$  system.

«Fig. 5 near here»

Two- and three-center  $\pi$ -only bond index values,  $W$  and  $Y$ , as well as the total energies and dipole moments, are reported in Table 3 for the various fixed-orbital combinations of the  $SC_x(10)$  components ( $x=c, d, I$ ). We observe that  $SC_c\oplus SC_I$  is the energetically preferred of the ‘binary’ combinations and that the  $\pi$ -only  $W$  and  $Y$  values, as well as the computed dipole moment, are considerably closer to the CASSCF(18,14) results than was the case for any of the separate  $SC_x(10)$  components. The relative weights of  $SC_c(10)$  and  $SC_I(10)$  in this  $SC_c\oplus SC_I$  combination are 62%:38% (Chirgwin-Coulson) or 69%:31% (Gallup-Norbeck).

We notice from Table 3 that although the energetically less favored  $SC_c\oplus SC_d$  and  $SC_d\oplus SC_I$  combinations turn out to be rather close to one another in terms of the total energy, the corresponding bond index and dipole moment values demonstrate that there are somewhat more substantial differences between these two constructions. This observation points to the possible utility of the combination of all three of the  $SC_x(10)$  components. As can be seen from Table 3, the energy lowering of the fixed-orbital  $SC_c\oplus SC_d\oplus SC_I$  construction relative to the  $SC_c\oplus SC_I$  combination is less than 4 millihartree but the  $\pi$ -only  $W$  and  $Y$  values and the computed dipole moment change in the second decimal place, mostly so as to be slightly closer to the corresponding CASSCF(18,14) values. We note that whereas the Chirgwin-Coulson weights in the  $SC_c\oplus SC_d\oplus SC_I$  combination are fairly similar to one another, being 35%, 34% and 31% for  $SC_c(10)$ ,  $SC_d(10)$  and  $SC_I(10)$ , respectively, the rival Gallup-Norbeck definition paints a somewhat different picture (19%, 11% and 70%, respectively), suggesting instead that  $SC_I(10)$  is more important in  $SC_c\oplus SC_d\oplus SC_I$  than it was in the  $SC_c\oplus SC_I$  construction.

Given that all of the various spin-coupling coefficients were treated as free parameters in these combinations of  $SC_x(10)$  components, it is important to check for any large changes in the preferred modes of spin coupling. This does indeed turn out to be the case. For example, we observe for the fixed-orbital  $SC_c \oplus SC_d \oplus SC_I$  combination that whereas the perfect-pairing mode ( $k = 42$  in the Kotani spin basis) accounts for more than 70% of the respective total spin functions for  $SC_d(10)$  and for each of the symmetry-related parts of  $SC_I(10)$ , the corresponding value for  $SC_c(10)$  is now just 18%. (For the latter component, the  $k = 28$  mode contributes 28%. This spin function, which corresponds to the path  $\alpha\beta\alpha\beta\alpha\beta\alpha\beta$  on the branching diagram (see Fig. 2), still represents perfect pairing for the spins of the  $\sigma$  electrons but, with this ordering of the orbitals, there are now two  $\pi$ -electron triplets (coupled, of course, to an overall singlet). The perfect-pairing mode accounts for 54% of the total spin function in the original  $SC_c(10)$  wavefunction.)

We subsequently attempted to generate various combinations of the  $SC_x(10)$  components in which all of the active orbitals were reoptimized. On the whole, such calculations proved difficult to converge, often with orbitals in different configurations starting to become nearly identical. Nevertheless, it is informative to mention briefly the fully-optimized  $SC_d \oplus SC_I$  combination, as an example of one of the more successful of these calculations. We found that the resulting symmetry-unique orbitals for the  $SC_I$ -like component do of course still exhibit the (enforced) asymmetry in the  $\pi$  space, but that the same is no longer so clear cut for the  $\sigma$  orbitals which, for the most part, are relatively similar to those for the (reoptimized)  $SC_d$ -like component. The Gallup-Norbeck weights are 33% and 67% for the  $SC_d$ -like and  $SC_I$ -like components, respectively. (Orbitals for the fully-optimized  $SC_d \oplus SC_I$  combination are depicted in Fig. S2 in the Supplementary Material.)

We observe from the various numerical values that are reported in Table 4 that whereas the fully-optimized  $SC_d \oplus SC_I$  combination performs well in terms of its total energy, the corresponding magnitudes of the  $\pi$ -only two- and three-center bond indices are somewhat smaller than those from the CASSCF(18,14) and corresponding icMRCI calculations (see Table 1). This suggests that the fully-optimized  $SC_d \oplus SC_I$  combination does not provide as good a description of the three-center four-electron bonding in the ozone  $\pi$  system as do these CASSCF(18,14) and icMRCI constructions or even, perhaps, as does the fixed-orbital  $SC_c \oplus SC_d \oplus SC_I$  combination. (As an aside, we note that the perfect-pairing mode of spin coupling dominates (at 89%) the  $SC_d$ -like component of the fully-optimized  $SC_d \oplus SC_I$  combination but that the corresponding value for each part of the  $SC_I$ -like component is 49%,

with the  $k=28$  mode accounting for 42%. The perfect-pairing contribution in each part of the original  $SC_I(10)$  wavefunction is 83%.)

All in all, little appears to have been achieved for the quality of the description of the  $\pi$  system by allowing the fully-optimized  $SC_d \oplus SC_I$  wavefunction to have so much flexibility for the active  $\sigma$  orbitals, in spite of a significant improvement in the total energy. With this in mind, we also examined a fully-variational  $SC_c \oplus SC_d \oplus SC_I$  combination that is based instead on a common set of active  $\sigma$  orbitals. The relative weights of the  $SC_c$ -like,  $SC_d$ -like and  $SC_I$ -like components are 44%:26%:30% (Chirgwin-Coulson) or 33%:35%:32% (Gallup-Norbeck), so that none of these three components dominates the total wavefunction. As can be seen from Table 4, the resulting energy of this orbital-relaxed common- $\sigma$  combination is lower than that of the fixed-orbital  $SC_c \oplus SC_d \oplus SC_I$  construction (Table 3) but, from the perspective of the  $\pi$ -only two- and three-center bond indices, it appears to offer much the same description of the  $\pi$  system as does the fully-optimized  $SC_d \oplus SC_I$  combination. (Orbitals for the fully-optimized  $SC_c \oplus SC_d \oplus SC_I$  combination based on a common set of active  $\sigma$  orbitals are depicted in Fig. S3 in the Supplementary Material. The perfect-pairing mode accounts for a fair proportion of the respective total spin functions for the  $SC_c$ -like component (74%) and for each of the symmetry-related parts of the  $SC_I$ -like component (nearly 58%); for the latter component, there is roughly 15% from each of  $k=28$  and  $k=41$ . The latter spin function, which corresponds to the path  $\alpha\alpha\beta\beta\alpha\beta\alpha\beta$  on the branching diagram (see Fig. 2), represents two  $\sigma$ -electron triplets (coupled to an overall singlet), for this ordering of the orbitals, but then perfect pairing for the remaining electron spins. The  $SC_d$ -like component of this fully-optimized  $SC_c \oplus SC_d \oplus SC_I$  combination behaves rather differently, in the sense that the perfect-pairing contribution drops substantially so as to be just 23%, whereas it is 89% in the original  $SC_d(10)$  wavefunction.)

#### 4. Conclusions

We expanded the  $\pi$  active space of the full-valence CASSCF description of  $O_3$  from  $2 \times B_1 + 1 \times A_2$  to  $3 \times B_1 + 2 \times A_2$  so as to encompass the corresponding  $2 \times B_1 + 2 \times A_2$  and  $3 \times B_1 + 1 \times A_2$   $\pi$  active spaces, respectively, for the rival  $SC_c$  and  $SC_d$  solutions. Domain-averaged Fermi hole analysis of the resulting CASSCF(18,14) construction suggests that the  $\pi$  system of ozone features three-center four-electron bonding, whereas the  $\sigma$  system is rather more ordinary, with a familiar pattern of fairly ordinary two-center two-electron O–O  $\sigma$  bonds and nonbonding  $\sigma$  orbitals. A similar picture emerges from an examination of

the LNOs generated by applying Cioslowski's isopycnic localization transformation [25] to the CASSCF(18,14) canonical natural orbitals. Moreover, much the same pattern of LNOs is observed for an icMRCI calculation that uses CASSCF(18,14) as its reference. Numerical values of two- and three-center bond indices for the CASSCF(18,14) wavefunction also turn out to be rather similar to those from the subsequent icMRCI calculation. This gives us the confidence to use such bond indices, alongside relative energies and the electric dipole moment, to assess the relative merits of different  $SC_x(10)$  components and of various combinations of them.

For the two-center bond index  $W_{AB}$  [13] we used a QTAIM generalization [30] of Mayer's improved definition of two-center bond orders for correlated singlet systems [29]. The sum of all possible  $W_{AB}$  values is equal to the total number of (active) electrons. The derivation of the expression for  $W_{AB}$  formally involves replacing the spin-density matrix  $\mathbf{P}^s$  by a particular matrix  $\mathbf{R}$  [29]; the use of much the same strategy for the corresponding three-center bond index leads to the definition of  $X_{ABC}$  in Eq. 9 [31, 32]. However, directly inspired by the simple form of the final expression for  $W_{AB}$  (Eq. 8) [13], we have instead introduced here a new three-center bond index, which we denote  $Y_{ABC}$  (see Eq. 12). Whereas it turns out to be true for various systems, including ozone, that the value of  $Y(A,B,C) = 3! Y_{ABC}$  for a given triad tends to be rather similar to that of  $X(A,B,C) = 3! X_{ABC}$ , our new definition does have the clear advantage that the sum of all possible  $Y_{ABC}$  values necessarily matches the total number of (active) electrons,  $N$ . The same is not true for  $X_{ABC}$ , although the deviation from  $N$  is often fairly small.

The  $\sigma$ -only bond order  $W_{12}$  between adjacent atoms is close to unity for the CASSCF(18,14) and subsequent icMRCI calculations, with the  $\sigma$ -only value of  $W_{23}$  (*i.e.* the bond order between the two terminal atoms) being much smaller. Although also fairly small, the magnitude (and sign) of the  $\sigma$ -only value of  $Y(O1,O2,O3)$  is suggestive of a small degree of three-center four-electron character in the  $\sigma$  framework. The  $\pi$  system is clearly rather different: the  $\pi$ -only  $W_{12}$  and  $W_{23}$  values are closer to one another and the magnitude of the (negative)  $\pi$ -only  $Y(O1,O2,O3)$  index is somewhat larger, corresponding to a significant degree of three-center four-electron  $\pi$  character, just as was suggested by the forms of the LNOs for these wavefunctions and by the results of the DAFH analysis. We observed that a  $\pi$ -only CASSCF(4,5) calculation, based on  $3 \times B_1 + 2 \times A_2$ , gives a particularly poor value for the dipole moment. Furthermore, we found that the  $\pi$ -only  $W_{AB}$  values and especially the  $\pi$ -only  $Y(O1,O2,O3)$  value can be rather sensitive to whether or not the  $\sigma$  system is treated as active in the wavefunction calculations, indicating that it was indeed important to increase the



number of active electrons in the various SC calculations from four ( $\pi$ -only) to ten. (Entirely analogous behavior was observed for the ‘full-valence’ sequence of CASSCF(4,3), CASSCF(18,12) and subsequent icMRCI calculations, and also when using values of  $X(O1,O2,O3)$  instead of those of  $Y(O1,O2,O3)$ .)

Earlier SC (or full-GVB) calculations for the ground state of  $O_3$  at its equilibrium geometry treated as active either four electrons (*i.e.*  $\pi$  only) [1-3] or eight electrons (four  $\pi$  and four  $\sigma$  bonding) [2]. We have extended such calculations to ten electrons in the present study, treating as active also the two nonbonding  $\sigma$  electrons associated with the central O atom. Whereas some authors have emphasized the importance of the  $SC_d$  type of description [2, 24], others have asserted that neither of the  $SC_c$  nor  $SC_d$  configurations provides a very satisfactory account on its own of the bonding in the  $\pi$  system [1, 3]. It does in fact turn out that  $SC_c(10)$  is energetically very slightly preferred over  $SC_d(10)$ . However, instead of focusing on fairly small energy differences, or picking one description over another according to its suitability for a particular type of explanation, we chose here to look instead at the two- and three-center bond indices for the  $\pi$  system and also at the electric dipole moment, thereby enabling direct comparison with the CASSCF(18,14) and icMRCI calculations. As well as the  $SC_c(10)$  and  $SC_d(10)$  wavefunctions, we generated an  $SC_I(10)$  construction that consists of a pair of symmetry-related pseudo-ionic configurations, each with its own set of suitably-polarized  $\sigma$  orbitals, so that it should have sufficient flexibility to encompass the model advocated by Kalemos and Mavridis [14, 15], were that to be energetically favored. After assessing each of these  $SC_x(10)$  ( $x=c, d, I$ ) components separately, we examined the qualities of various combinations of them, with or without subsequent orbital reoptimization.

Given the apparently relatively ordinary nature of the  $\sigma$  system, it made most sense when assessing the quality of the various VB wavefunctions to focus on the variations in the  $\pi$ -only bond indices. We found that the performance of the  $SC_c(10)$  and  $SC_d(10)$  wavefunctions for the quantities that we monitored most closely matches that of the  $\pi$ -only CASSCF(4,5) calculation, except for improved total energies and, in the case of  $SC_d(10)$ , a slightly better estimate of the dipole moment. Comparing the various  $SC_x(10)$  values with those from the CASSCF(18,14) and icMRCI calculations, we observe that only the  $SC_I(10)$  construction gives good estimates of the  $\pi$ -only bond indices. On the other hand, not only is the dipole moment greatly overestimated by the  $SC_I(10)$  wavefunction, but the total energy is so poor that we have to conclude that this description is totally inadequate on its own. It did, however, turn out to be useful in fixed-orbital combinations with  $SC_c(10)$  and especially with

$SC_d(10)$ . According to the direct comparison with the CASSCF(18,14) and icMRCI two- and three-center  $\pi$ -only bond indices, there is relatively little to choose between the quality of the fixed-orbital  $SC_d \oplus SC_I$  and  $SC_c \oplus SC_d \oplus SC_I$  combinations, although the latter does appear to yield a somewhat better estimate of the dipole moment. (Note that although the orbitals are fixed, there is significant relaxation of some of the spin-coupling coefficients.) On the whole, various subsequent orbital optimizations resulted, rather disappointingly, in somewhat inferior  $\pi$ -only  $Y(O1,O2,O3)$  indices, in spite of some significant improvements in the total energy. According to the majority of our multi-component VB constructions, the weight of the  $SC_d$  type of description in the total wavefunction is on the order of  $1/3$ .

The description of the  $\pi$  system which emerges from all of our various forms of analysis conforms, perhaps unsurprisingly, to a standard model of three-center four-electron  $\pi$  bonding that incorporates a nontrivial degree of (partial) diradical character. Using mostly the values of the new three-center bond index  $Y(A,B,C)$  to judge their relative qualities, we find that certain combinations of the  $SC_x(10)$  ( $x = c, d, I$ ) components can faithfully reproduce such a picture of the  $\pi$  bonding, whereas none of the individual  $SC_x(10)$  wavefunctions appears to be have sufficient flexibility on its own.

## **Appendix A. Supplementary material**

Supplementary data associated with this article can be found, in the online version, at [⟨DOI⟩](#).

## References

- [1] T. Thorsteinsson, D.L. Cooper, J. Gerratt, P.B. Karadakov, M. Raimondi, Modern valence bond representations of CASSCF wavefunctions, *Theor. Chim. Acta*, 93 (1996) 343-366.
- [2] T.Y. Takeshita, B.K. Lindquist, T.H. Dunning, Insights into the electronic structure of ozone and sulfur dioxide from generalized valence bond theory: Bonding in O<sub>3</sub> and SO<sub>2</sub>, *J. Phys. Chem. A*, 119 (2015) 7683-7694.
- [3] F.E. Penotti, D.L. Cooper, Combining rival  $\pi$ -space descriptions of O<sub>3</sub> and of SO<sub>2</sub>, *Int. J. Quantum Chem.*, 116 (2016) 718-730.
- [4] R. Ponec, Electron pairing and chemical bonds. Chemical structure, valences and structural similarities from the analysis of the Fermi holes, *J. Math. Chem.*, 21 (1997) 323-333.
- [5] R. Ponec, Electron pairing and chemical bonds. Molecular structure from the analysis of pair densities and related quantities, *J. Math. Chem.*, 23 (1998) 85-103.
- [6] R. Ponec, A.J. Duben, Electron pairing and chemical bonds: Bonding in hypervalent molecules from analysis of Fermi holes, *J. Comput. Chem.*, 20 (1999) 760-771.
- [7] R. Ponec, J. Roithová, Domain-averaged Fermi holes - a new means of visualization of chemical bonds. Bonding in hypervalent molecules, *Theor. Chem. Acc.*, 105 (2001) 383-392.
- [8] R. Ponec, D.L. Cooper, A. Savin, Analytic models of domain-averaged Fermi holes: A new tool for the study of the nature of chemical bonds, *Chem. Eur. J.*, 14 (2008) 3338-3345.
- [9] P. Bultinck, D.L. Cooper, R. Ponec, Influence of atoms-in-molecules methods on shared-electron distribution indices and domain-averaged Fermi Holes, *J. Phys. Chem. A*, 114 (2010) 8754-8763.
- [10] D. Tiana, E. Francisco, M.A. Blanco, P. Macchi, A. Sironi, Á.M. Pendás, Restoring orbital thinking from real space descriptions: bonding in classical and non-classical transition metal carbonyls, *PCCP*, 13 (2011) 5068-5077.
- [11] A.I. Baranov, R. Ponec, M. Kohout, Domain-averaged Fermi-hole analysis for solids, *J. Chem. Phys.*, 137 (2012).
- [12] E. Francisco, Á.M. Pendás, A. Costales, On the interpretation of domain averaged Fermi hole analyses of correlated wavefunctions, *PCCP*, 16 (2014) 4586-4597.

- [13] D.L. Cooper, R. Ponec, M. Kohout, New insights from domain-averaged Fermi holes and bond order analysis into the bonding conundrum in C<sub>2</sub>, *Mol. Phys.*, 114 (2016) 1270-1284.
- [14] A. Kalemios, A. Mavridis, Electronic structure and bonding of ozone, *J. Chem. Phys.*, 129 (2008) 054312.
- [15] A. Kalemios, Comment on "Insights into the Electronic Structure of Ozone and Sulfur Dioxide from Generalized Valence Bond Theory: Bonding in O<sub>3</sub> and SO<sub>2</sub>", *J. Phys. Chem. A*, 120 (2016) 169-170.
- [16] T.H. Dunning, T.Y. Takeshita, B.A. Lindquist, Reply to "Comment on 'Insights into the Electronic Structure of Ozone and Sulfur Dioxide from Generalized Valence Bond Theory: Bonding in O<sub>3</sub> and SO<sub>2</sub>'", *J. Phys. Chem. A*, 120 (2016) 171-172.
- [17] V.A. Glezakou, S.T. Elbert, S.S. Xantheas, K. Ruedenberg, Analysis of bonding patterns in the valence isoelectronic series O<sub>3</sub>, S<sub>3</sub>, SO<sub>2</sub>, and OS<sub>2</sub> in terms of oriented quasi-atomic molecular orbitals, *J. Phys. Chem. A*, 114 (2010) 8923-8931.
- [18] E. Miliordos, K. Ruedenberg, S.S. Xantheas, Unusual inorganic biradicals: A theoretical analysis, *Angew. Chem. Int. Ed.*, 52 (2013) 5736-5739.
- [19] E. Miliordos, S.S. Xantheas, On the Bonding Nature of Ozone (O-3) and Its Sulfur-Substituted Analogues SO<sub>2</sub>, OS<sub>2</sub>, and S-3: Correlation between Their Biradical Character and Molecular Properties, *J. Am. Chem. Soc.*, 136 (2014) 2808-2817.
- [20] A. DeBlase, M. Licata, J.M. Galbraith, A Valence Bond Study of Three-Center Four-Electron  $\pi$  Bonding: Electronegativity vs Electroneutrality, *J. Phys. Chem. A*, 112 (2008) 12806-12811.
- [21] Y. Lan, S.E. Wheeler, K.N. Houk, Extraordinary difference in reactivity of ozone (OOO) and sulfur dioxide (OSO): A Theoretical study, *J. Chem. Theory Comput.*, 7 (2011) 2104-2111.
- [22] R.D. Harcourt, *Bonding in Electron-Rich Molecules: Qualitative Valence-Bond Approach via Increased-Valence Structures*, 2nd Edition, Springer-Verlag, Berlin, 2016.
- [23] R.D. Harcourt, T.M. Klapotke, Comment on "A quantitative definition of hypervalency" by M. C. Durrant, *Chem. Sci.*, 2015, 6, 6614, *Chem. Sci.*, 7 (2016) 3443-3447.
- [24] B.A. Lindquist, T.Y. Takeshita, T.H. Dunning, Insights into the Electronic Structure of Ozone and Sulfur Dioxide from Generalized Valence Bond Theory: Addition of Hydrogen Atoms, *J. Phys. Chem. A*, 120 (2016) 2720-2726.

- [25] J. Cioslowski, Isopycnic orbital transformation and localization of natural orbitals, *Int. J. Quantum Chem.*, S24 (1990) 15-28.
- [26] R.F.W. Bader, *Atoms in Molecules. A Quantum Theory*, Oxford University Press, Oxford, 1990.
- [27] R. Pauncz, *The Symmetric Group in Quantum Chemistry*, CRC Press, Boca Raton, 1995.
- [28] I. Mayer, *Bond orders and energy components: Extracting chemical information from molecular wave functions*, CRC Press, Boca Raton, 2017.
- [29] I. Mayer, Improved definition of bond orders for correlated wave functions, *Chem. Phys. Lett.*, 544 (2012) 83-86.
- [30] J.G. Ángyán, M. Loos, I. Mayer, Covalent bond orders and atomic valence indices in the topological theory of atoms in molecules, *J. Phys. Chem.*, 98 (1994) 5244-5248.
- [31] D.L. Cooper, R. Ponec, Insights into molecular electronic structure from domain averaged Fermi hole (DAFH) and bond order analysis using correlated density matrices, in: R. Carbó-Dorca, T. Chakraborty (Eds.) *Theoretical & Quantum Chemistry at the Dawn's End of 21<sup>st</sup> Century*, Apple Academic Press, New Jersey, 2017 (in press).
- [32] R. Ponec, D.L. Cooper, Peculiarities of Be(0) bonding in the light of modern computational analysis, submitted for publication.
- [33] H.J. Werner, P.J. Knowles, A 2nd order multiconfiguration SCF procedure with optimum convergence, *J. Chem. Phys.*, 82 (1985) 5053-5063.
- [34] P.J. Knowles, H.J. Werner, An efficient 2nd order MC SCF method for long configuration expansions, *Chem. Phys. Lett.*, 115 (1985) 259-267.
- [35] H.J. Werner, P.J. Knowles, An efficient internally contracted multiconfiguration-reference configuration interaction method, *J. Chem. Phys.*, 89 (1988) 5803-5814.
- [36] P.J. Knowles, H.J. Werner, An efficient method for the evaluation of coupling coefficients in configuration interaction calculations, *Chem. Phys. Lett.*, 145 (1988) 514-522.
- [37] H.-J. Werner, P.J. Knowles, G. Knizia, F.R. Manby, M. Schütz, Molpro: a general-purpose quantum chemistry program package, *WIREs Comput. Mol. Sci.*, 2 (2012) 242-253.
- [38] H.-J. Werner, P.J. Knowles, G. Knizia, F.R. Manby, M. Schütz, P. Celani, W. Györffy, D. Kats, T. Korona, R. Lindh, A. Mitrushenkov, G. Rauhut, K.R. Shamasundar, T.B. Adler, R.D. Amos, A. Bernhardsson, A. Berning, D.L. Cooper, M.J.O. Deegan, A.J. Dobbyn, F. Eckert, E. Goll, C. Hampel, A. Hesselmann, G. Hetzer, T. Hrenar, G. Jansen,

- C. Köppl, Y. Liu, A.W. Lloyd, R.A. Mata, A.J. May, S.J. McNicholas, W. Meyer, M.E. Mura, A. Nicklass, D.P. O'Neill, P. Palmieri, D. Peng, K. Pflüger, R. Pitzer, M. Reiher, T. Shiozaki, H. Stoll, A.J. Stone, R. Tarroni, T. Thorsteinsson, M. Wang, MOLPRO, version 2015.1, a package of ab initio programs, Cardiff, U. K., see [www.molpro.net](http://www.molpro.net).
- [39] T.A. Keith, AIMAll (Version 13.11.04), TK Gristmill Software, Overland Park KS, USA, see [aim.tkgristmill.com](http://aim.tkgristmill.com).
- [40] F.E. Penotti, The optimized-basis-set multiconfiguration spin-coupled method for the ab initio calculation of atomic and molecular electronic wave functions, *Int. J. Quantum Chem.*, 46 (1993) 535-576.
- [41] F.E. Penotti, Generalization of the optimized-basis-set multi-configuration spin-coupled method for the ab initio calculation of atomic and molecular electronic wave functions, *Int. J. Quantum Chem.*, 59 (1996) 349-378.
- [42] F.E. Penotti, On the identification of symmetry-forbidden spin subspaces for configurations employing nonorthogonal orbitals, *Int. J. Quantum Chem.*, 78 (2000) 24-31.
- [43] F.E. Penotti, Orbital-orthogonality constraints and basis-set optimization, *J. Comput. Chem.*, 27 (2006) 762-772.
- [44] M.W. Schmidt, K.K. Baldridge, J.A. Boatz, S.T. Elbert, M.S. Gordon, J.H. Jensen, S. Koseki, N. Matsunaga, K.A. Nguyen, S.J. Su, T.L. Windus, M. Dupuis, J.A. Montgomery, General atomic and molecular electronic-structure system, *J. Comput. Chem.*, 14 (1993) 1347-1363.
- [45] M.S. Gordon, M.W. Schmidt, Advances in electronic structure theory: GAMESS a decade later, *Theory and Applications of Computational Chemistry: The First Forty Years*, 2005, pp. 1167-1189.
- [46] D.R. Lide, *CRC Handbook of Chemistry and Physics*, 85 ed., CRC Press, Boca Raton, 2005.
- [47] B.H. Chirgwin, C.A. Coulson, The electronic structure of conjugated systems. VI, *Proc. R. Soc. London, A*, 201 (1950) 196-209.
- [48] G.A. Gallup, J.M. Norbeck, Population analyses of valence-bond wavefunctions and BeH<sub>2</sub>, *Chem. Phys. Lett.*, 21 (1973) 495-500.
- [49] G. Schaftenaar, J.H. Noordik, Molden: a pre- and post-processing program for molecular and electronic structures, *J. Comput. Aided Mol. Des.*, 14 (2000) 123-134.
- [50] R. Ponec, I. Mayer, Investigation of some properties of multicenter bond indices, *J. Phys. Chem. A*, 101 (1997) 1738-1741.

- [51] T. Kar, E. Sánchez Marcos, Three-center four-electron bonds and their indices, *Chem. Phys. Lett.*, 192 (1992) 14-20.
- [52] J.F. Stanton, J. Gauss, M.E. Harding, P.G. Szalay, with contributions from A.A. Auer, R.J. Bartlett, U. Benedikt, C. Berger, D.E. Bernholdt, Y. Bomble, *et al.*, CFOUR, Coupled-Cluster techniques for Computational Chemistry, a quantum-chemical program package, see [www.cfour.de](http://www.cfour.de).

**Table 1**

Two- and three-center bond index values ( $W$  and  $Y$ ), total energies ( $E$ ) and dipole moments ( $\mu$ ) for various CASSCF and icMRCI wavefunctions that are described in the text. These icMRCI calculations are based on a CASSCF(18,14) reference.

Quantity	CASSCF(4,5)	CASSCF(18,14)	icMRCI
$W_{12}$ $\sigma$ -only		1.077	1.067
$W_{12}$ $\pi$ -only	0.386	0.426	0.417
$W_{12}$		1.503	1.485
$W_{23}$ $\sigma$ -only		0.144	0.146
$W_{23}$ $\pi$ -only	0.188	0.240	0.237
$W_{23}$		0.383	0.383
$Y(\text{O1},\text{O2},\text{O3})$ $\sigma$ -only		-0.028	-0.026
$Y(\text{O1},\text{O2},\text{O3})$ $\pi$ -only	-0.092	-0.141	-0.142
$Y(\text{O1},\text{O2},\text{O3})$		-0.169	-0.168
$E$ / hartree	-224.47534	-224.63469	-225.15086
$\mu$ / debye	0.288	0.505	0.510



**Table 2**

Two- and three-center bond index values ( $W$  and  $Y$ ), total energies ( $E$ ) and dipole moments ( $\mu$ ) for the various  $SC_x(10)$  wavefunctions that are described in the text.

Quantity	$SC_c(10)$	$SC_d(10)$	$SC_l(10)$
$W_{12}$ $\pi$ -only	0.396	0.370	0.428
$W_{23}$ $\pi$ -only	0.186	0.188	0.235
$Y(O1,O2,O3)$ $\pi$ -only	-0.098	-0.084	-0.141
$E$ / hartree	-224.54286	-224.53633	-224.47739
$\mu$ / debye	0.245	0.380	1.411

**Table 3**

Two- and three-center bond index values ( $W$  and  $Y$ ), total energies ( $E$ ) and dipole moments ( $\mu$ ) for various fixed-orbital combinations of  $SC_x(10)$  configurations, as described in the text.

Quantity	$SC_c \oplus SC_d$	$SC_c \oplus SC_I$	$SC_d \oplus SC_I$	$SC_c \oplus SC_d \oplus SC_I$
$W_{12}$ $\pi$ -only	0.391	0.437	0.432	0.426
$W_{23}$ $\pi$ -only	0.186	0.266	0.238	0.256
$Y(O1,O2,O3)$ $\pi$ -only	-0.096	-0.152	-0.145	-0.144
$E$ / hartree	-224.55586	-224.56634	-224.55511	-224.57001
$\mu$ / debye	0.401	0.564	0.634	0.518

**Table 4**

Two- and three-center bond index values ( $W$  and  $Y$ ), total energy ( $E$ ) and dipole moment ( $\mu$ ) for fully-optimized  $SC_d \oplus SC_I$  and  $SC_c \oplus SC_d \oplus SC_I$  combinations, with the latter based on a common set of active  $\sigma$  orbitals.

Quantity	$SC_d \oplus SC_I$	$SC_c \oplus SC_d \oplus SC_I$
$W_{12}$ $\pi$ -only	0.403	0.406
$W_{23}$ $\pi$ -only	0.201	0.207
$Y(O1,O2,O3)$ $\pi$ -only	-0.116	-0.114
$E$ / hartree	-224.59855	-224.57850
$\mu$ / debye	0.539	0.477

## Figure captions

### Figure 1

Selected Lewis-like structures for O<sub>3</sub>.

### Figure 2

Branching diagram for the visualization of Kotani spin functions. The values in the circles are the total numbers of spin functions for each allowed combination of  $N$  and  $S$ .

### Figure 3

CASSCF(18,14) LNOs and occupation numbers for ozone. Symmetry-related counterparts are identified in parentheses.

### Figure 4

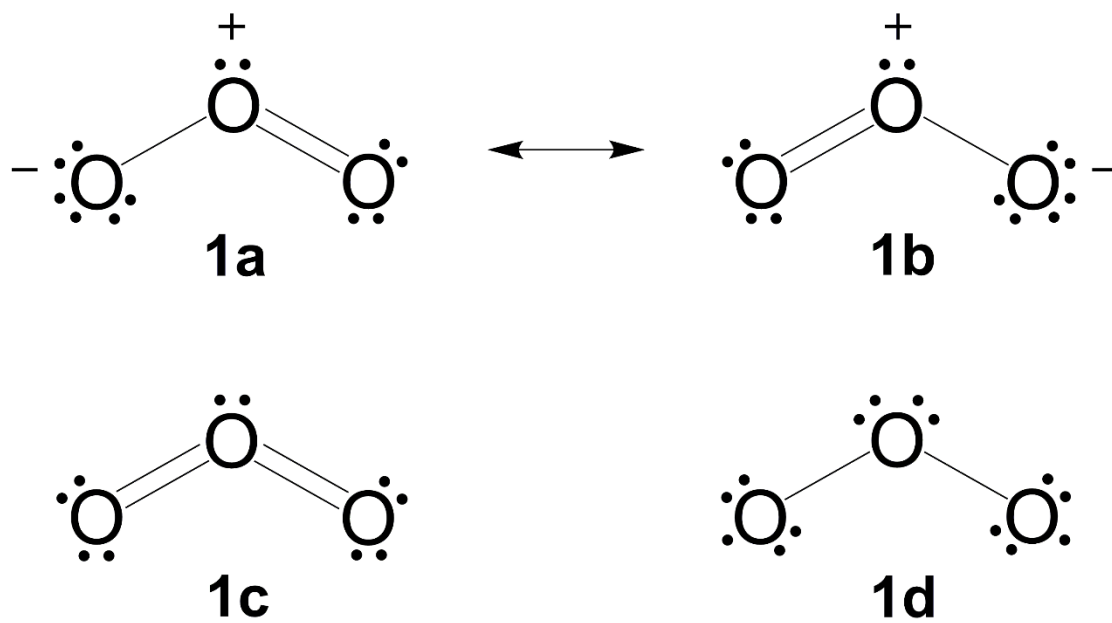
CASSCF(18,14) DAFH functions and occupation numbers for the domain of the central atom O1 (first column) and for the domain of terminal atom O2 (second column).

Symmetry-related counterparts within these domains are identified in parentheses.

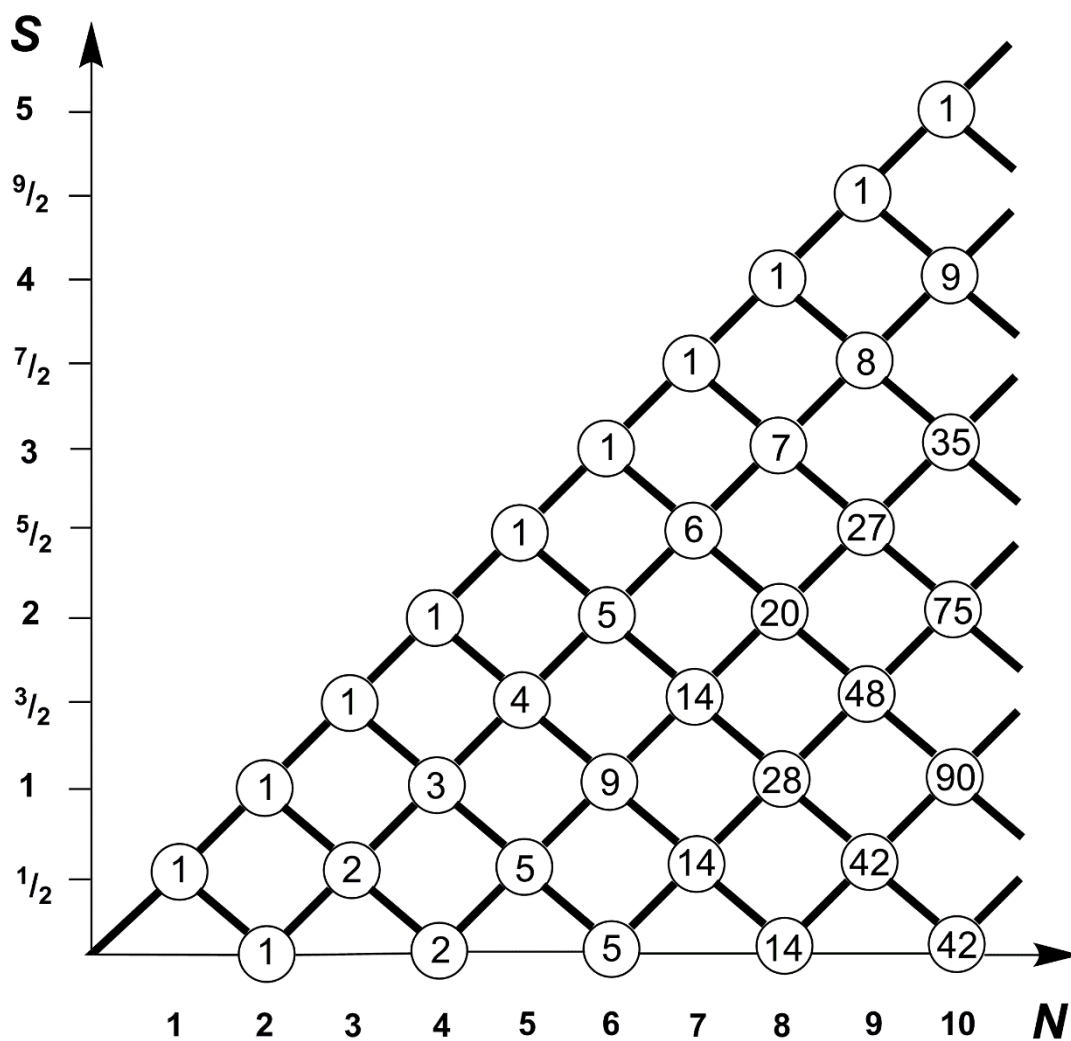
### Figure 5

Active orbitals from separate spin-coupled calculations for ozone: SC<sub>c</sub>(10), top two rows, SC<sub>d</sub>(10), middle two rows, and SC<sub>f</sub>(10), final two rows. Only the symmetry-unique orbitals have been shown in the case of SC<sub>f</sub>(10).

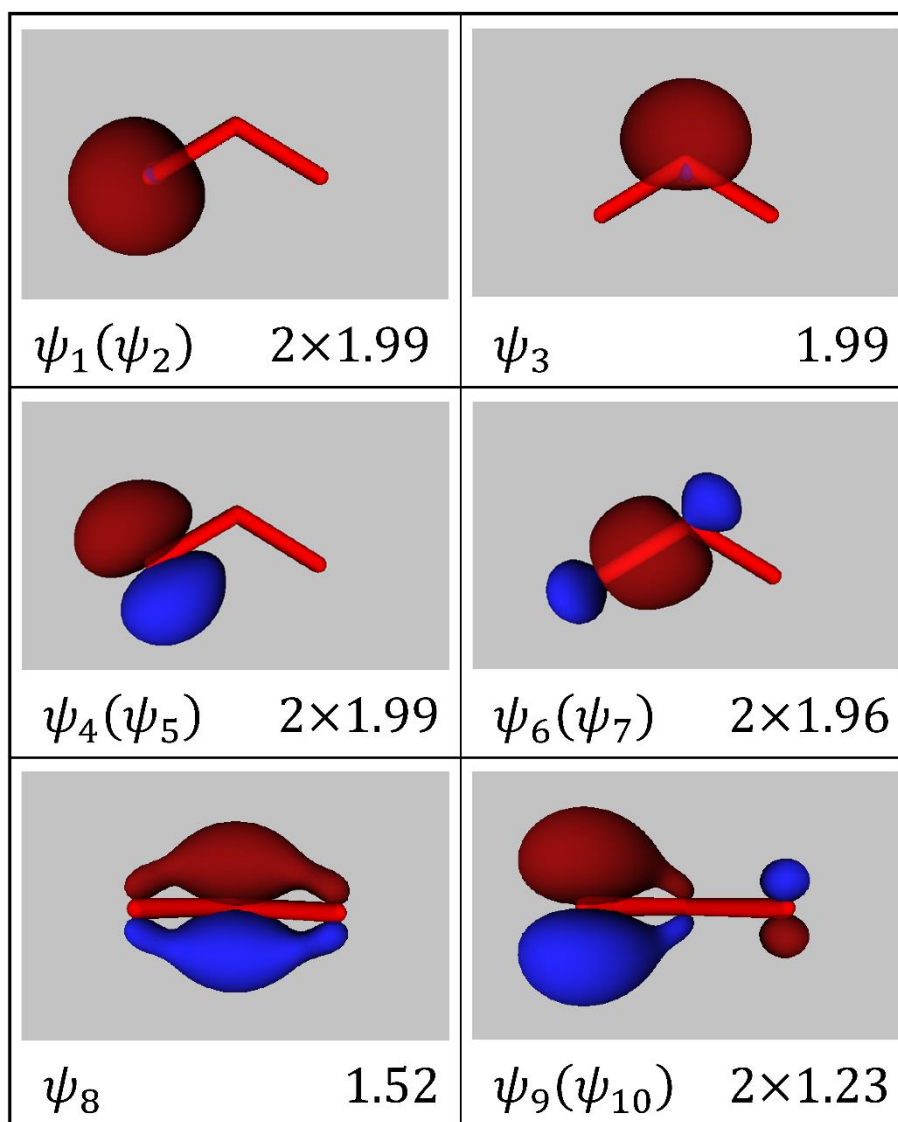
**Fig. 1.** Selected Lewis-like structures for O<sub>3</sub>.



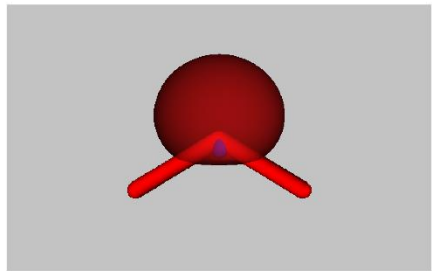
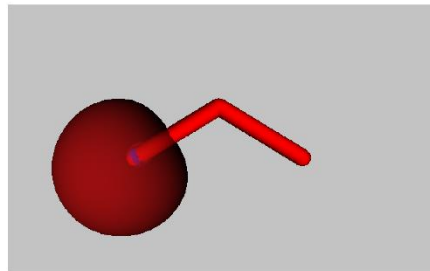
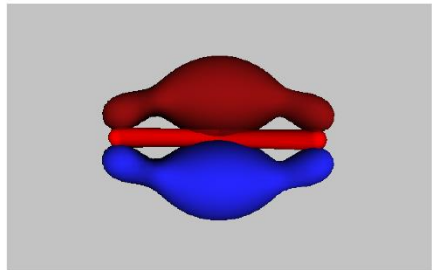
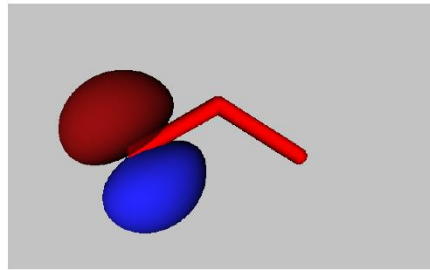
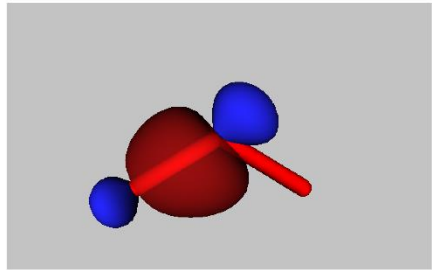
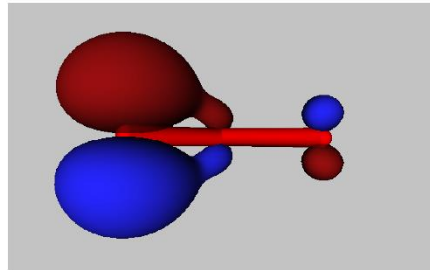
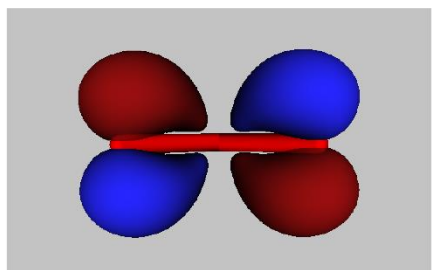
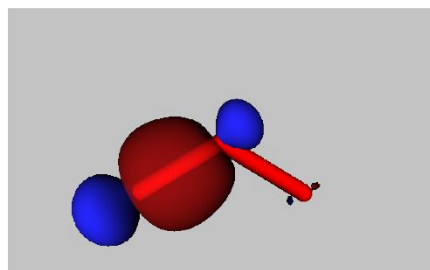
**Fig. 2.** Branching diagram for the visualization of Kotani spin functions. The values in the circles are the total numbers of spin functions for each allowed combination of  $N$  and  $S$ .



**Fig. 3 – color for online version.** CASSCF(18,14) LNOs and occupation numbers for ozone. Symmetry-related counterparts are identified in parentheses.

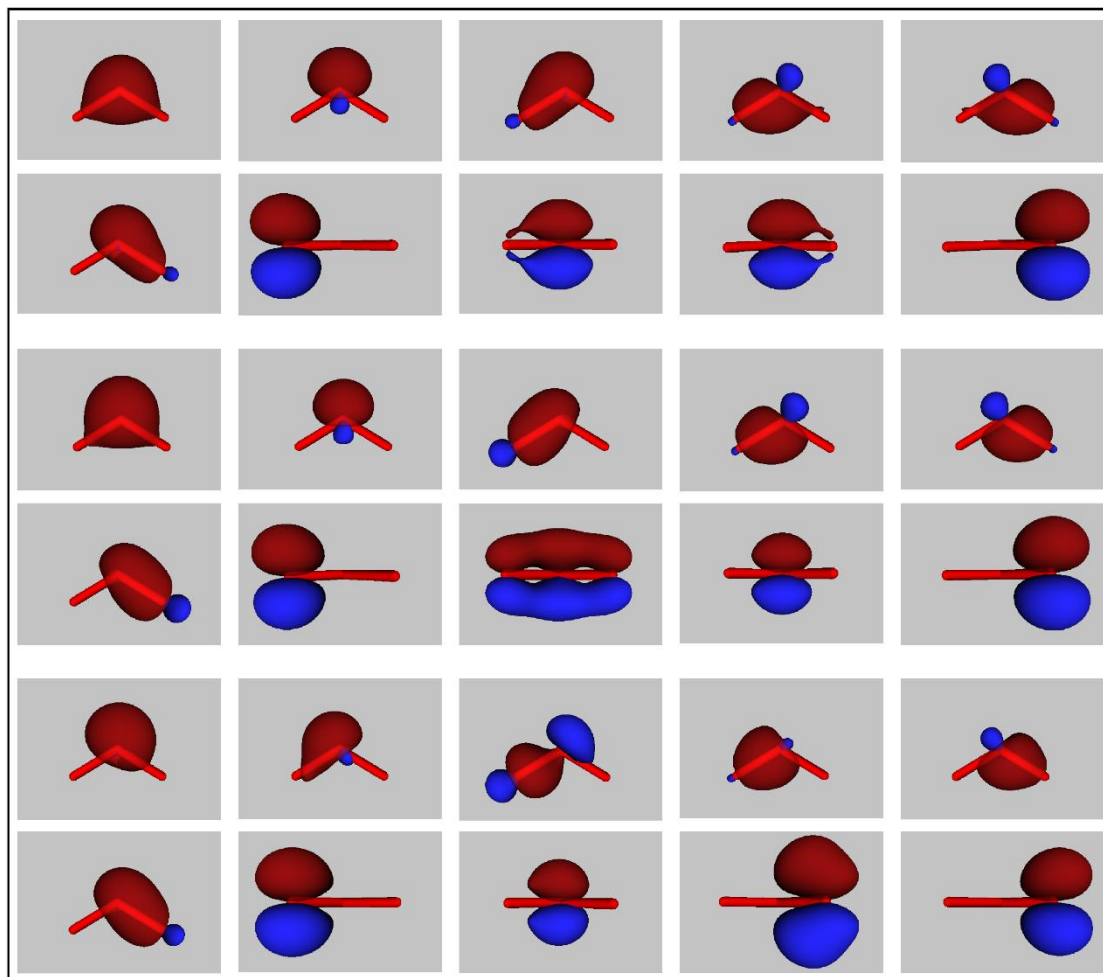


**Fig. 4 – color.** CASSCF(18,14) DAFH functions and occupation numbers for the domain of the central atom O1 (first column) and for the domain of terminal atom O2 (second column). Symmetry-related counterparts within these domains are identified in parentheses.

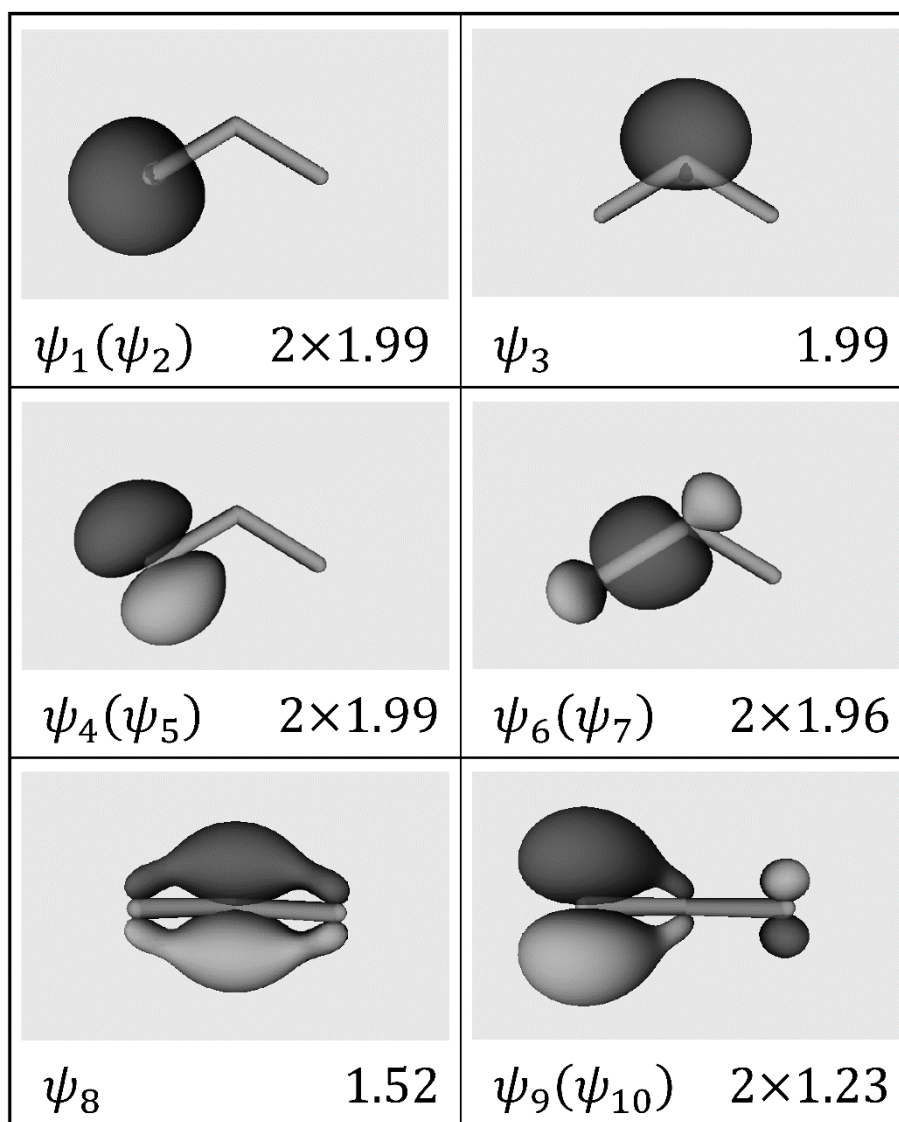
O1	O2
 $\varphi_1^{O1}$ 1.95	 $\varphi_1^{O2}$ 1.98
 $\varphi_2^{O1}$ 1.35	 $\varphi_2^{O2}$ 1.89
 $\varphi_3^{O1} (\varphi_4^{O1})$ $2 \times 1.13$	 $\varphi_3^{O2}$ 1.21
 $\varphi_5^{O1}$ 0.14	 $\varphi_4^{O2}$ 0.91



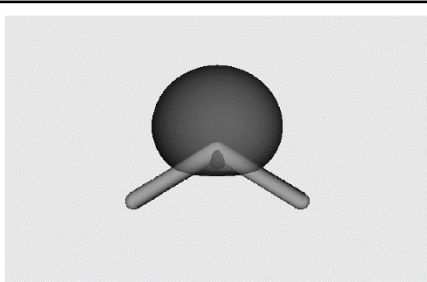
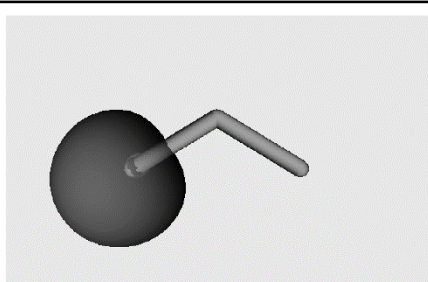
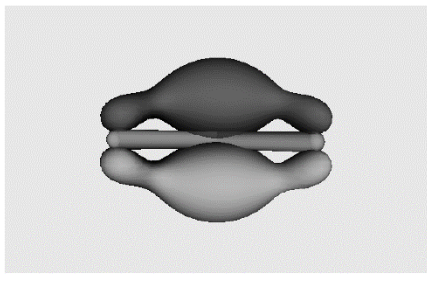
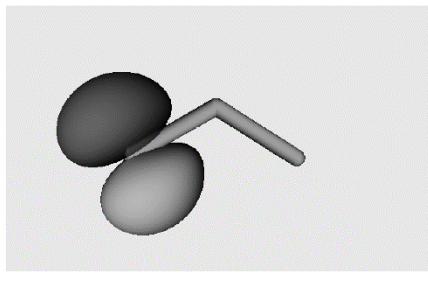
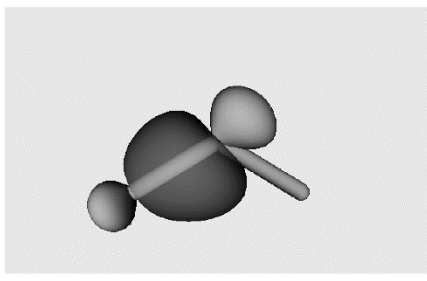
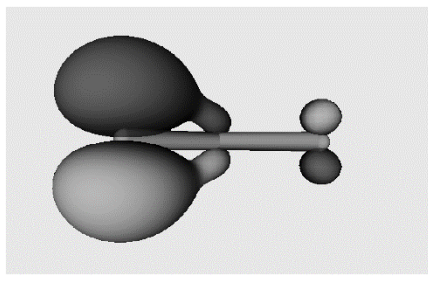
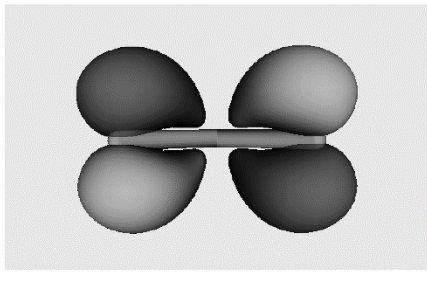
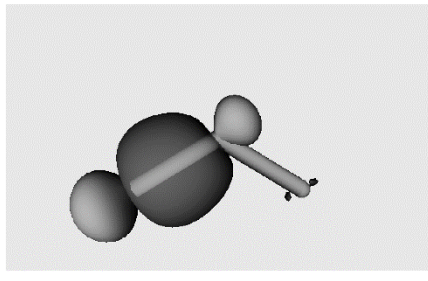
**Fig. 5 – color for online version.** Active orbitals from separate spin-coupled calculations for ozone:  $SC_c(10)$ , top two rows,  $SC_d(10)$ , middle two rows, and  $SC_f(10)$ , final two rows. Only the symmetry-unique orbitals have been shown in the case of  $SC_f(10)$ .



**Fig. 3 – b/w for printed version.** CASSCF(18,14) LNOs and occupation numbers for ozone. Symmetry-related counterparts are identified in parentheses.



**Fig. 4 – b/w.** CASSCF(18,14) DAFH functions and occupation numbers for the domain of the central atom O1 (first column) and for the domain of terminal atom O2 (second column). Symmetry-related counterparts within these domains are identified in parentheses.

O1	O2
 $\varphi_1^{O1}$ 1.95	 $\varphi_1^{O2}$ 1.98
 $\varphi_2^{O1}$ 1.35	 $\varphi_2^{O2}$ 1.89
 $\varphi_3^{O1} (\varphi_4^{O1})$ $2 \times 1.13$	 $\varphi_3^{O2}$ 1.21
 $\varphi_5^{O1}$ 0.14	 $\varphi_4^{O2}$ 0.91

**Fig. 5 – b/w for printed version.** Active orbitals from separate spin-coupled calculations for ozone:  $SC_c(10)$ , top two rows,  $SC_d(10)$ , middle two rows, and  $SC_f(10)$ , final two rows. Only the symmetry-unique orbitals have been shown in the case of  $SC_f(10)$ .

